M.V. Moroz[1], P.Yu. Demchenko[2], F. Tesfaye[3, 4], M.V. Prokhorenko[5], O.I. Mysina[1], L.V. Soliak[1], N.P. Yarema[5], S.V. Prokhorenko[5], O.V. Reshetnyak[2]

Thermodynamic properties of selected compounds of the Ag–In–Se system determined by the electromotive force method

[1]National University of Water and Environmental Engineering, Rivne, 33028, Ukraine, m.v.moroz@nuwm.edu.ua
[2]Ivan Franko National University of Lviv, Lviv, 79005, Ukraine
[3]Åbo Akademi University, Turku, 20500, Finland
[4]Metso Outotec Finland Oy, Espoo, 02231, Finland
[5]Lviv Polytechnic National University, Lviv,79013, Ukraine

The equilibrium phase space of the Ag–In–Se system in the part $AgInSe_2$–$InSe$–Se below 500 K consists seven three-phase regions In_2Se_3–$AgIn_{11}Se_{17}$–Se (I), $AgIn_{11}Se_{17}$–$AgIn_5Se_8$–Se (II), $AgIn_5Se_8$–$AgInSe_2$–Se (III), In_2Se_3–In_6Se_7–$AgIn_{11}Se_{17}$ (IV), In_6Se_7–$AgIn_{11}Se_{17}$–$AgIn_5Se_8$ (V), $InSe$–In_6Se_7–$AgIn_5Se_8$, and $InSe$–$AgIn_5Se_8$–$AgInSe_2$ (VI). Division of the $AgInSe_2$–$InSe$–Se into separate phase regions was performed based on electromotive force vs temperature dependences of six electrochemical cells (ECCs) of the type: $(-)$ C | Ag | SE | R(Ag$^+$) | PE | C (+), where C is the graphite (inert electrode), Ag is the left (negative) electrode, SE is the solid-state electrolyte (Ag_3GeS_3Br glass), PE is the right (positive) electrode, R(Ag$^+$) is the buffer region of PE that contacts with SE. The process of forming of the thermodynamically stable set of phases from phase non-equilibrium mixture of compounds specified in (I)–(VI) is carried out in the R(Ag$^+$) region. The Ag$^+$ ions act as the small nucleation centers for stable phases. Based on the temperature dependences of the electromotive force of ECCs with PE of the (I)–(VI) phase regions, the standard thermodynamic functions of the binary In_6Se_7 and three ternary compounds in the adjacent phase regions were calculated for the first time. The agreement of the calculated values of the standard Gibbs energies of the $AgIn_5Se_8$ compound in two different phase regions (II) and (V): $\Delta_f G^\circ_{(II)} = -(819.6 \pm 8.9)$ kJ·mol^{-1} and $\Delta_f G^\circ_{(V)} = -(820.0 \pm 8.9)$ kJ·mol^{-1} characterizes the phase composition of the regions (I), (II), (IV), and (V) below 500 K as a combination of compounds of formulaic composition.

Keywords: Ag-containing compounds, Thermodynamic properties, Phase equilibria, Gibbs energy, EMF method.

Introduction

The *T*–*x* diagram Ag_2Se–In_2Se_3 of the Ag–In–Se system features the formation of $AgInSe_2$, $AgIn_5Se_8$, and $AgIn_{11}Se_{17}$ compounds with congruent 1060 K, 1088 K, and incongruent 1077 K type of melting, respectively [1]. The $AgInSe_2$ and $AgIn_5Se_8$ compounds crystallize from the melt as phases of variable composition, undergo polymorphic transformations at 968 K and 1013 K, respectively. The homogeneity ranges of these compounds are equal ~3 and ~4 mol.% In_2Se_3 at the room temperature. The isothermal cross-section of the Ag–In–Se system at 723 K is characterized by the Ag_3In, Ag_2Se, In_4Se_3, $InSe$, In_6Se_7, In_2Se_3, $AgInSe_2$, and $AgIn_5Se_8$ compounds [2]. The existence of $AgIn_{11}Se_{17}$ compound has not been established. The ternary $AgInSe_2$ and $AgIn_5Se_8$ compounds are evaluated as promising for use in nonlinear optics, manufacturing of visible and infrared LEDs, infrared detectors, solar cells, and other electro-optical devices [3,4]. Information on the main thermodynamic properties of the ternary phases $AgInSe_2$ and $AgIn_5Se_8$, which are important for the analysis of uncontrolled changes in the operation of scientific and technological equipment, is currently lacking. Presented

in [5,6] data on the standard Gibbs energy of the formation of AgInSe$_2$ and AgIn$_5$Se$_8$ compounds $\Delta_fG^\circ = -188$ kJ·mol^{-1} and $\Delta_fG^\circ = -850$ kJ·mol^{-1} are approximate because they do not take into account the Gibbs energy of the synthesis reactions Δ_rG° from the calculated amounts of Ag$_2$Se and In$_2$Se$_3$.

The purpose of this work was to establish the values of standard thermodynamic functions (Gibbs energy, enthalpy, and entropy) of the AgInSe$_2$, AgIn$_5$Se$_8$, AgIn$_{11}$Se$_{17}$, and In$_6$Se$_7$ compounds by using the EMF method [7–9] and literature data on the thermodynamic properties of the InSe and In$_2$Se$_3$ compounds [10]. The results of calculations of thermodynamic functions of compounds can be used to analyze the reasons for changes in the performance of equipment manufactured with their participation and modeling the phase diagrams of multicomponent systems, including Ag–In–Se, by the CALPHAD methods [11,12].

I. Experimental

The high purity elements Ag, In, and Se (>99.99 wt.%, Alfa Aesar, Germany) were used for synthesis of the compounds. The evacuated melts of the calculated amounts of the elements were well-mixed for 20 min and followed by cooling to the room temperature at a rate of ~5 K·min^{-1}. Crushed to a particle size of ~5 μm polycrystalline samples were used for X-ray analysis and preparation of positive electrodes of electrochemical cells (ECCs). An STOE STADI P diffractometer equipped with a linear position-sensitive detector PSD, in a Guinier geometry (transmission mode, CuKα$_1$ radiation, a bent Ge(111) monochromator, and 2θ/ω scan mode) was used to establish the phase composition of the samples. The following programs STOE WinXPOW [13], PowderCell [14], FullProf [15], as well as databases [16,17] were used for X-ray phase analysis.

Synthesis of a thermodynamically equilibrium set of compounds below 500 K from a phase non-equilibrium mixture of compounds obtained by cooling the melts and the EMF (E) measurements were performed in ECCs type (A):

$$(-)C|Ag|SE|R(Ag^+)|PE|C(+), \qquad (A)$$

where C is the graphite (inert electrode), Ag is the left (negative) electrode, SE is the solid-state electrolyte (Ag$_3$GeS$_3$Br glass), PE is the right (positive) electrode, R(Ag$^+$) is the buffer region of PE that contacts with SE. The process of forming of the thermodynamically stable set of phases from phase non-equilibrium mixture of finely dispersed compounds is carried out in the R(Ag$^+$) region. The Ag$^+$ ions act as the small nucleation centers for stable phases [18].

Components of the ECCs in powder form were pressed at 10^8 Pa through a 2 mm diameter hole arranged in fluoroplast matrix up to density $\rho = (0.93 \pm 0.02)\cdot\rho_0$, where ρ_0 is the experimentally determined density of cast samples [19,20]. The experiments were performed in a horizontal resistance furnace, similar to that described in [21]. As the protection atmosphere we used a flow of highly purified (99.99 volume fraction) Ar (g) at $P = 1.2\cdot10^5$ Pa. The gas flow of Ar at the rate of 10^{-5} m^3·min^{-1} from the right to the left electrodes of the ECCs. The temperature was maintained with an accuracy of $\pm$ 0.5 K. The EMF values of the cells were measured using high-resistance (input impedance of >10^{12} Ω) the Picotest M3500A universal digital multimeter. The equilibrium in ECCs at each temperature was achieved within 2 h. During equilibrium the EMF values were constant or their variations were not exceed $\pm$0.2 mV [22]. The dependences of the EMF of the cells on temperature $E(T)$ were analyzed by the method described in [23–25]. The ratios of initials components of PE of ECCs were determined from the equations of potential-forming reactions in respective phase regions.

II. Results and discussion

The alleged scheme division of the concentration space of the Ag–In–Se system in the AgInSe$_2$–InSe–Se region below 500 K, confirmed our investigations of the boundaries of the phase fields by the EMF method, is shown in Fig. 1.
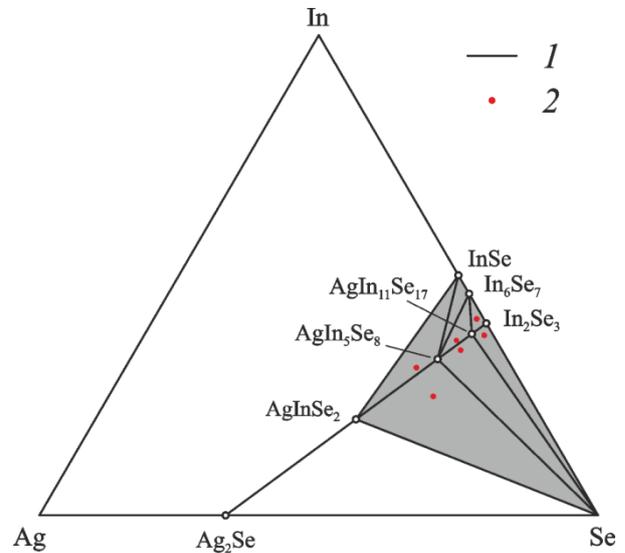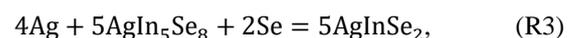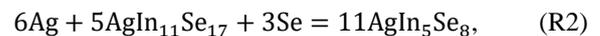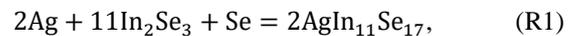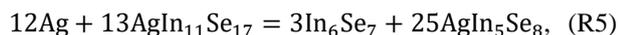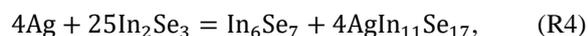

Fig. 1. Division of the concentration space of the Ag–In–Se system in the AgInSe$_2$–InSe–Se region below 500 K: *1* are lines of two-phase equilibria, *2* are compositions of the positive electrodes of the ECCs in the phase regions (I)–(VI).

The position of the three-phase regions: In$_2$Se$_3$–AgIn$_{11}$Se$_{17}$–Se (I), AgIn$_{11}$Se$_{17}$–AgIn$_5$Se$_8$–Se (II), AgIn$_5$Se$_8$–AgInSe$_2$–Se (III), In$_2$Se$_3$–AgIn$_{11}$Se$_{17}$–In$_6$Se$_7$ (IV), In$_6$Se$_7$–AgIn$_{11}$Se$_{17}$–AgIn$_5$Se$_8$ (V), InSe–In$_6$Se$_7$–AgIn$_5$Se$_8$, and InSe–AgIn$_5$Se$_8$–AgInSe$_2$ (VI) relative to silver was used to write equations of the overall potential-forming reactions:

$$2Ag + 11In_2Se_3 + Se = 2AgIn_{11}Se_{17}, \qquad (R1)$$

$$6Ag + 5AgIn_{11}Se_{17} + 3Se = 11AgIn_5Se_8, \qquad (R2)$$

$$4Ag + 5AgIn_5Se_8 + 2Se = 5AgInSe_2, \qquad (R3)$$

$$4Ag + 25In_2Se_3 = In_6Se_7 + 4AgIn_{11}Se_{17}, \qquad (R4)$$

$$12Ag + 13AgIn_{11}Se_{17} = 3In_6Se_7 + 25AgIn_5Se_8, \quad (R5)$$

$$2Ag + AgIn_5Se_8 = 2InSe + 3AgInSe_2. \qquad (R6)$$

Equations (R1)–(R6) were used to establish the ratios of selenium, binary and ternary compounds in PE of ECCs.

The cooled melts of the binary and ternary compounds mentioned in reactions (R1)–(R6) are thermodynamically non-equilibrium. In particular, according to results of X-ray analysis, the cooled melt of the formula composition

In_2Se_3 is characterized by two modifications of In_2Se_3 with closely related structures (space groups (SG) $P6_3$ for the In_2Se_3 phase, stable under normal conditions, and SG $P6_1$ for the high-temperature modification of In_2Se_3), and the InSe sample, apart from the InSe compound (SG $R3m$), contains impurities of the In_6Se_7 phase (SG $P2_1/m$), Fig. 2, a, b. The crystallized $AgIn_{11}Se_{17}$ melt contains a set of lines of the $AgIn_{11}Se_{17}$ compound with an uncertain structure and the $AgIn_5Se_8$ (SG P-$42m$), Fig. 2, c. The crystallized $AgIn_5Se_8$ contains impurities of the $AgInSe_2$, Fig. 2, d. Alloys of the formulas In_6Se_7 and $AgIn_5Se_8$ crystallize as single-phase samples.

Newly assembled PE of the ECCs according to

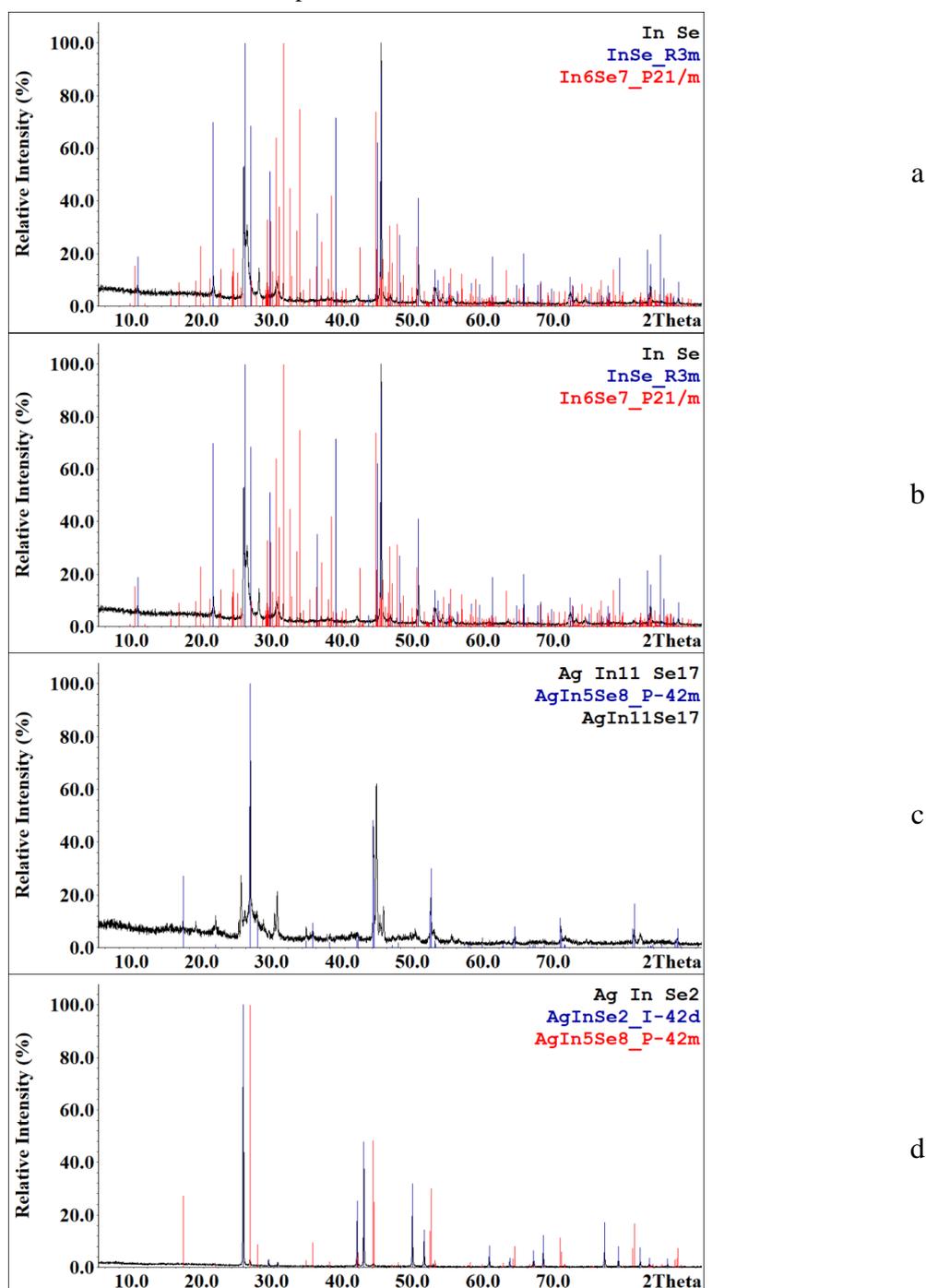**Fig. 2.** X-ray powder diffraction patterns of samples with composition: In_2Se_3 (a), InSe (b), $AgIn_{11}Se_{17}$ (c), and $AgInSe_2$ (d) (black color). Compositions of the samples and identified phases (with space group indicated) are shown in the upper right corner.

equations (R1)–(R6) are the combination of thermodynamically nonequilibrium phases, which cause the formation of the R(Ag$^+$) region in the ECC. The process of forming of the thermodynamically stable set of phases from phase non-equilibrium mixture of finely dispersed compounds for the participation of Ag$^+$ ions as a catalyst end in 48 hours at 500 K. The criterion for attaining phase equilibria in the R(Ag$^+$) region of PE is the reproducibility of the $E(T)$ relations of ECCs during the heating-cooling cycles.

The measured EMF values as a function temperature of ECCs are presented in Table 1.

A summary of the measured EMF values and temperatures of ECCs from the phase regions (I)–(VI).

T/K	Phase regions					
	(I)	(II)	(III)	(IV)	(V)	(VI)
	E/mV	E/mV	E/mV	E/mV	E/mV	E/mV
430.3	375.1	367.7	362.3	385.7	374.7	364.8
435.2	375.6	368.4	362.9	386.4	375.2	365.2
440.2	376.0	368.9	363.3	387.0	375.8	365.7
445.2	376.3	369.6	363.9	387.7	376.3	366.1
450.1	376.7	370.2	364.4	388.5	376.9	366.6
455.1	377.1	370.9	365.2	389.2	377.5	367.0
460.0	377.5	371.5	365.7	389.9	378.0	367.4
465.0	377.9	372.1	366.1	390.5	378.5	367.9
469.9	378.2	372.7	366.7	391.2	379.1	368.3
474.7	378.6	373.4	367.4	391.9	379.7	368.8
479.3	379.0	374.1	367.8	392.6	380.3	369.3
484.0	379.4	374.7	368.4	393.3	380.9	369.8
489.6	379.9	375.5	368.9	393.9	381.4	370.2
494.5	*380.7**	376.1	369.7	394.7	381.9	370.6

* Data point not included in treatment

The linear dependencies $E(T)$ between 430 K and 494 K provided that $\Delta_r C_p$ = const and equal zero [23] were calculated by the least squares method and expressed as:

$$E_{(R1)}/\text{mV} = (341.2 \pm 0.3) + (78.8 \pm 0.7) \cdot 10^{-3} T/\text{K}, \quad (1)$$

$$E_{(R2)}/\text{mV} = (311.3 \pm 0.5) + (130.9 \pm 1.0) \cdot 10^{-3} T/\text{K}, \quad (2)$$

$$E_{(R3)}/\text{mV} = (313.2 \pm 0.6) + (114.1 \pm 1.3) \cdot 10^{-3} T/\text{K}, \quad (3)$$

$$E_{(R4)}/\text{mV} = (325.3 \pm 0.4) + (140.3 \pm 0.8) \cdot 10^{-3} T/\text{K}, \quad (4)$$

$$E_{(R5)}/\text{mV} = (325.6 \pm 0.4) + (113.9 \pm 0.9) \cdot 10^{-3} T/\text{K}, \quad (5)$$

$$E_{(R6)}/\text{mV} = (325.3 \pm 0.4) + (91.6 \pm 0.8) \cdot 10^{-3} T/\text{K}. \quad (6)$$

The temperature dependences the EMF of ECCs is presented in Fig. 3.

The correctness of presented in Fig. 1 division of the Ag–In–Se system in the AgInSe$_2$–InSe–Se part below 500 K is confirmed by the following provisions:

E vs T dependences of ECCs with PE of the (I)–(VI) phase regions are characterized by different EMF values at T=const and the intercept and slope coefficients;

the phase regions that are more distant from the point of Ag are characterized by higher EMF values at T = const.
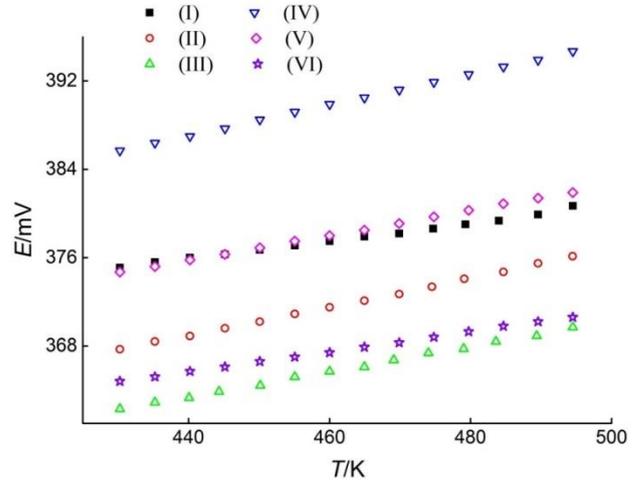

Fig. 3. Temperature dependences of EMF (E) vs temperature (T) of the ECCs with positive electrodes of the phase regions (I)–(VI).

The Gibbs energies, enthalpies, and entropies of reactions (R1)–(R6) can be calculated by applying the thermodynamic Eqs. (7)–(9):

$$\Delta_r G = -z \cdot \text{F} \cdot E, \quad (7)$$

$$\Delta_r H = -z \cdot \text{F} \cdot [E - (dE/dT) \cdot T], \quad (8)$$

$$\Delta_r S = z \cdot \text{F} \cdot (dE/dT), \quad (9)$$

where z is the number of electrons involved in the reactions (R1)–(R6), F = 96485.33289 C·mol^{-1} is Faraday's constant, and E is the EMF of ECCs.

The values of thermodynamic functions of the reactions (R1)–(R6) at 298 K and p=10^5 Pa were calculated using Eqs. (7)–(9). The determined results are listed in Table 2.

The Gibbs energy, enthalpy, and entropy of reaction (R1) are related to the Gibbs energy, enthalpy, and entropy of the AgInSe$_2$ compound and pure elements of Ag and Se by Eqs. (10)–(12):

The values of standard thermodynamic functions of the reactions (R1)–(R6).

Reaction	$-\Delta_r G^\circ$	$-\Delta_r H^\circ$	$\Delta_r S^\circ$
	kJ·mol^{-1}		J·(mol·K)$^{-1}$
(R1)	70.37 ± 0.74	65.84 ± 1.99	15.20 ± 2.18
(R2)	202.80 ± 1.92	180.22 ± 2.25	75.78 ± 2.53
(R3)	134.00 ± 1.06	120.88 ± 2.16	44.04 ± 1.33
(R4)	141.69 ± 1.18	125.55 ± 2.20	54.15 ± 1.24
(R5)	416.31 ± 3.54	376.99 ± 4.58	131.88 ± 2.71
(R6)	68.04 ± 0.59	62.77 ± 1.09	17.68 ± 0.61

$$\Delta_{r(R1)}G^{\circ} = 2\Delta_{f}G^{\circ}_{AgIn_{11}Se_{17}} - 11\Delta_{f}G^{\circ}_{In_{2}Se_{3}}, \tag{10}$$

$$\Delta_{r(R1)}H^{\circ} = 2\Delta_{f}H^{\circ}_{AgIn_{11}Se_{17}} - 11\Delta_{f}H^{\circ}_{In_{2}Se_{3}}, \tag{11}$$

$$\Delta_{r(R1)}S^{\circ} = 2S^{\circ}_{AgIn_{11}Se_{17}} - 2S^{\circ}_{Ag} - 11S^{\circ}_{In_{2}Se_{3}} - S^{\circ}_{Se}. \tag{12}$$

It follows from Eqs. (10)–(12) that:

$$\Delta_{f}G^{\circ}_{AgIn_{11}Se_{17}} = 0{,}5\left(11\Delta_{f}G^{\circ}_{In_{2}Se_{3}} + \Delta_{r(R1)}G^{\circ}\right), \tag{13}$$

$$\Delta_{f}H^{\circ}_{AgIn_{11}Se_{17}} = 0{,}5\left(11\Delta_{f}H^{\circ}_{In_{2}Se_{3}} + \Delta_{r(R1)}H^{\circ}\right), \tag{14}$$

$$S^{\circ}_{AgIn_{11}Se_{17}} = 0{,}5\left(2S^{\circ}_{Ag} + 11S^{\circ}_{In_{2}Se_{3}} + S^{\circ}_{Se} + \Delta_{r(R1)}S^{\circ}\right). \tag{15}$$

Similarly, the corresponding equations to determine $\Delta_{f}G^{\circ}$, $\Delta_{f}H^{\circ}$, and S° of the $AgIn_5Se_8$, $AgInSe_2$, In_6Se_7, $AgIn_5Se_8$, and $AgInSe_2$ compounds in the phase regions (II)–(VI) can be written based on reactions (R2)–(R6), with their appropriate stochiometric numbers.

Combining Eqs. (13)–(15), using thermodynamic data of the pure elements Ag, In, Se and binary compounds InSe, In_2Se_3 [10], the standard thermodynamic data of selected compounds in the Ag–In–Se system were calculated for the first time. A comparative summary of the calculated values together with the available literature data is listed in Table 3.

The coincidence of the calculated values of the thermodynamic functions of the compound $AgIn_5Se_8$ in the phase sections (II), (V) characterizes the phase composition (I), (II), (IV), (V) below 500 K as a combination of compounds of formulaic composition. The difference in the values of the thermodynamic properties of $AgInSe_2$ equilibrium in the phase regions (III), (VI) characterizes the ternary compound as a phase of variable composition.

Considering data presented in Table 3, the temperature dependences of the Gibbs energy of formation of the $AgIn_{11}Se_{17}$, $AgIn_5Se_8$, $AgInSe_2$, In_6Se_7, $AgIn_5Se_8$, and $AgInSe_2$ compounds in the phase regions (I)–(VI) are described by Eqs. (16)–(21), respectively:

$$\Delta_{f}G_{AgIn_{11}Se_{17},(I)}/(kJ \cdot mol^{-1}) = -(1827.8 \pm 20.3) + (218.8 \pm 3.1) \cdot 10^{-3}T/K, \tag{16}$$

$$\Delta_{f}G_{AgIn_{5}Se_{8},(II)}/(kJ \cdot mol^{-1}) = -(847.2 \pm 10.7) + (92.6 \pm 1.6) \cdot 10^{-3}T/K, \tag{17}$$

$$\Delta_{f}G_{AgInSe_{2},(III)}/(kJ \cdot mol^{-1}) = -(193.6 \pm 3.2) + (9.7 \pm 0.2) \cdot 10^{-3}T/K, \tag{18}$$

$$\Delta_{f}G_{In_{6}Se_{7},(IV)}/(kJ \cdot mol^{-1}) = -(973.0 \pm 11.3) + (100.0 \pm 1.7) \cdot 10^{-3}T/K, \tag{19}$$

$$\Delta_{f}G_{AgIn_{5}Se_{8},(V)}/(kJ \cdot mol^{-1}) = -(848.8 \pm 10.9) + (96.5 \pm 1.6) \cdot 10^{-3}T/K, \tag{20}$$

$$\Delta_{f}G_{AgInSe_{2},(VI)}/(kJ \cdot mol^{-1}) = -(224.7 \pm 4.3) + (12.7 \pm 0.3) \cdot 10^{-3}T/K. \tag{21}$$

Table 3.

Values of standard thermodynamic functions of selected compounds of the Ag–In–Se system at T=298 K

Phase	Phase region	$-\Delta_{f}G^{\circ}$	$-\Delta_{f}H^{\circ}$	S°	Reference
		kJ·mol^{-1}		J·(mol·K)$^{-1}$	
Ag	–	0	0	42.677	[10]
In	–	0	0	57.823	[10]
Se	–	0	0	42.258	[10]
InSe	–	112.475	117.989	81.588	[10]
In$_2$Se$_3$	–	314.077	326.352	201.25	[10]
In$_6$Se$_7$	(IV)	943.2±9.4	973.0±11.3	542.8±9.2	This work
AgIn$_{11}$Se$_{17}$	(I)	1762.6±18.0	1827.8±20.3	1178.3±16.7	This work
AgInSe$_2$	(III)	190.7±2.1	193.6±3.2	175.3±4.1	This work
AgInSe$_2$	(VI)	220.9±2.8	224.7±4.3	172.3±3.9	This work
AgIn$_5$Se$_8$	(II)	819.6±8.9	847.2±10.7	577.3±9.8	This work
AgIn$_5$Se$_8$	(V)	820.0±8.9	848.8±10.9	573.3±9.7	This work

Conclusions

The phase composition and triangulation of the equilibrium *T-x* space of the Ag–In–Se system in the part of AgInSe$_2$–InSe–Se below 500 K have been established. The AgInSe$_2$–InSe–Se concentration space contains seven three-phase regions formed by the InSe, In$_6$Se$_7$, In$_2$Se$_3$, AgInSe$_2$, AgIn$_5$Se$_8$, and AgIn$_{11}$Se$_{17}$ compounds. Equations of the temperature dependences of the Gibbs energy as well as the values of standard thermodynamic functions of the In$_6$Se$_7$, AgInSe$_2$, AgIn$_5$Se$_8$, and AgIn$_{11}$Se$_{17}$ compounds were established for the first time. The phase composition of the InSe–AgIn$_5$Se$_8$–In$_6$Se$_7$, In$_6$Se$_7$–AgIn$_{11}$Se$_{17}$–AgIn$_5$Se$_8$, In$_2$Se$_3$–AgIn$_{11}$Se$_{17}$–In$_6$Se$_7$, In$_2$Se$_3$–AgIn$_{11}$Se$_{17}$–Se, and AgIn$_{11}$Se$_{17}$–AgIn$_5$Se$_8$–Se regions is a combination of stochiometric compounds.

Moroz M.V. – Doctor of Chemical Sciences, Professor of the department of chemistry and physics of the National University of Water and Environmental Engineering;
Demchenko P.Yu. – Ph. D. in Chemistry, Leading Researcher of the department of inorganic chemistry of Ivan Franko Lviv National University of Lviv;
Tesfaye F. – Doctor of Technical Sciences, Senior Researcher at the Laboratory of Molecular Science and Engineering, Åbo Akademi University, Finland;
Prokhorenko M.V. – Ph. D. in Physical and Mathematical Sciences, Associate Professor of the department of Cartography and Geospatial Modeling of the Lviv Polytechnic National University;
Mysina O.I. – Senior Lecturer of the department of chemistry and physics of the National University of Water and Environmental Engineering;
Solyak L.V. – Senior Lecturer of the department of chemistry and physics of the National University of Water and Environmental Engineering;
Yarema N.P. – Ph. D. in Technical Sciences, Associate Professor of the department of Cartography and Geospatial Modeling of the Lviv Polytechnic National University;
Prokhorenko S.V. – Doctor of Technical Sciences, Professor of the department of information and measurement technologies of the Lviv Polytechnic National University;
Reshetnyak O.V. – Doctor of Chemical Sciences, Head of the department of physical and colloidal chemistry of Ivan Franko National University of Lviv.

[1] I.D. Olekseyuk, O.V. Krykhovets, *The Ag$_2$Se–In$_2$Se$_3$–SnSe$_2$ System*, J. Alloys Compd., 316, 193 (2001); https://doi.org/10.1016/S0925-8388(00)01283-4.

[2] S. Chen, J. Chang, S. Tseng, et al. *Phase Diagrams of the Ag–In–Se Photovoltaic Material System*, J. Alloys Compd., 656, 58 (2016); https://doi.org/10.1016/j.jallcom.2015.09.206.

[3] T. Çolakoğlu, M. Parlak, *Structural Characterization of Polycrystalline Ag–In–Se Thin Films Deposited by e-Beam Technique*, Appl. Surf. Sci., 254, 1569 (2008); https://doi.org/10.1016/j.apsusc.2007.07.092.

[4] L. Jataute, V. Krylova, N. Dukštiene, M. Lelis, S. Tučkute, *Ag-In-Se Films on Flexible Architectural Textiles as Efficient Material for Optoelectronics Applications: A Preliminary Study*, Thin Solid Films, 721, 138566 (2021); https://doi.org/10.1016/j.tsf.2021.138566.

[5] L. Peraldo Bicelli, *Thermodynamic Evaluation of the N-AgIn$_5$Se$_8$ and n-CuIn$_5$S$_8$ Stability in Photoelectrochemical Cells, Solar Energy Materials*, 15, 77 (1987); https://doi.org/10.1016/0165-1633(87)90084-0.

[6] L. Peraldo Bicelli, *Thermodynamic Stability of Silver Indium Selenide (n-AgInSe$_2$) in Photoelectrochemical Cells*, J. Phys. Chem., 92(24), 6991 (1988); https://doi.org/10.1021/j100335a030.

[7] G.S. Hasanova, A.I. Aghazade, Y.A. Yusibov, M.B. Babanly, *Thermodynamic Properties of the BiTe and Bi$_8$Te$_9$ Compounds*, Physics and Chemistry of Solid State, 21(4), 714 (2020); https://doi.org/10.15330/pcss.21.4.714-719.

[8] S.Z. Imamaliyeva, I.F. Mehdiyeva, D.B. Taghiyev, M.B. Babanly, *Thermodynamic Investigations of the Erbium Tellurides by EMF Method*, Physics and Chemistry of Solid State, 21(2), 312 (2020); https://doi.org/10.15330/pcss.21.2.312-318.

[9] T.M. Alakbarova, E.N. Orujlu, D.M. Babanly, S.Z. Imamaliyeva, M.B. Babanly, *Solid-Phase Equilibria in the GeBi$_2$Te$_4$-Bi$_2$Te$_3$-Te System and Thermodynamic Properties of Compounds of the GeTe·mBi$_2$Te$_3$ Homologous Series*, Physics and Chemistry of Solid State, 23(1), 25 (2022); https://doi.org/10.15330/pcss.23.1.25-33.

[10] I. Barin, *Thermochemical Data of Pure Substances* (Wiley, 1995).

[11] A. Kroupa, *Modelling of Phase Diagrams and Thermodynamic Properties Using Calphad Method – Development of Thermodynamic Databases*, Comput. Mater. Sci., 66, 3 (2013); http://dx.doi.org/10.1016/j.commatsci.2012.02.003.

[12] B. Sundman, Q. Chen, Y. Du, *A Review of Calphad Modeling of Ordered Phases*, J. Phase Equilib. Diffus., 39, 678 (2018); https://doi.org/10.1007/s11669-018-0671-y.

[13] Diffractometer Stoe WinXPOW, version 3.03 (Stoe & Cie GmbH, Darmstadt, 2010).

[14] W. Kraus, G. Nolze, *POWDER CELL – a Program for the Representation and Manipulation of Crystal Structures and Calculation of the Resulting X-Ray Powder Patterns*, J. Appl. Crystallogr., 29(3), 301 (1996); https://doi.org/10.1107/S0021889895014920.

[15] J. Rodriguez-Carvajal, *Recent Developments of the Program FULLPROF*. IUCr Commission on Powder Diffraction Newsletter, 26, 12 (2001).

[16] R.T. Downs, M. Hall-Wallace, *The American Mineralogist Crystal Structure Database*, Am. Mineral., 88(1), 247 (2003).

[17] P. Villars and K. Cenzual, *Pearson's Crystal Data: Crystal Structure Database for Inorganic Compounds*, Release 2014/15, ASM International: Materials Park. OH, USA, 2014.

[18] M. Moroz, F. Tesfaye, P. Demchenko, M. Prokhorenko, S. Prokhorenko, O. Reshetnyak, *Non-Activation Synthesis and Thermodynamic Properties of Ternary Compounds of the Ag–Te–Br System*, Thermochim. Acta, 698, 178862 (2021); https://doi.org/10.1016/j.tca.2021.178862.

[19] M.V. Prokhorenko, M.V. Moroz, P.Yu. Demchenko, *Measuring the Thermodynamic Properties of Saturated Solid Solutions in the Ag_2Te-Bi-Bi_2Te_3 System by the Electromotive Force Method*, Russ. J. Phys. Chem. A., 89, 1330 (2015); https://doi.org/10.1134/S0036024415080269.

[20] M.V. Moroz, P.Yu. Demchenko, M.V. Prokhorenko, O.V. Reshetnyak, *Thermodynamic Properties of Saturated Solid Solutions of the Phases Ag_2PbGeS_4, $Ag_{0.5}Pb_{1.75}GeS_4$ and $Ag_{6.72}Pb_{0.16}Ge_{0.84}S_{5.20}$ of the Ag-Pb-Ge-S System Determined by EMF Method*, J. Phase Equilib. Diffus., 38, 426 (2017); https://doi.org/10.1007/s11669-017-0563-6.

[21] F. Tesfaye, P. Taskinen, Electrochemical Study of the *Thermodynamic Properties of Matildite (β-$AgBiS_2$) in Different Temperature and Compositional Ranges*, J. Solid State Electrochem., 18, 1683 (2014); https://doi.org/10.1007/s10008-014-2395-1.

[22] M. Moroz, F. Tesfaye, P. Demchenko, M. Prokhorenko, D. Lindberg, O. Reshetnyak, L. Hupa, *Phase Equilibria and Thermodynamics of Selected Compounds in the Ag–Fe–Sn–S System*, J. Electron. Mater., 47, 5433 (2018); https://doi.org/10.1007/s11664-018-6430-3.

[23] E.G. Osadchii, O.A. Rappo, *Determination of Standard Thermodynamic Properties of Sulfides in the Ag-Au-S System by Means of a Solid-State Galvanic Cell*, Am. Mineral., 89, 1405 (2004); https://doi.org/10.2138/am-2004-1007.

[24] G.S. Hasanova, A.I. Aghazade, S.Z. Imamaliyeva, Y.A. Yusibov, M.B. Babanly, *Refinement of the Phase Diagram of the Bi-Te System and the Thermodynamic Properties of Lower Bismuth Tellurides*, JOM, 73, 1511 (2021); https://doi.org/10.1007/s11837-021-04621-1.

[25] G.S. Hasanova, A.I. Aghazade, D.M. Babanly, S.Z. Imamaliyeva, Y.A. Yusibov, M.B. Babanly, *Experimental Study of the Phase Relations and Thermodynamic Properties of Bi-Se System*, J. Therm. Anal. Calorim., 147, 6403 (2022); https://doi.org/10.1007/s10973-021-10975-0.

М.В. Мороз[1], П.Ю. Демченко[2], Ф. Тесфає[3, 4], М.В. Прохоренко[5], О.І. Мисіна[1], Л.В. Соляк[1], Н.П. Ярема[5], С.В. Прохоренко[5], О.В. Решетняк[2]

Термодинамічні властивості окремих сполук системи Ag–In–Se, визначені методом електрорушійних сил

[1]Національний університет водного господарства та природокористування, вул. Соборна, 11, 33028 Рівне, Україна, m.v.moroz@nuwm.edu.ua
[2]Львівський національний університет імені Івана Франка, вул. Кирила і Мефодія, 6, 79005 Львів, Україна
[3]Університет Академія Або, Піісканкату, 8, 20500 Турку, Фінляндія
[4]Метсо Оутотек Фінланд, Раухаланпуісто, 9, 02231 Еспо, Фінляндія
[5]Національний університет "Львівська політехніка", вул. Степана Бандери, 12, 79013 Львів, Україна

Рівноважний *T–x* простір системи Ag–In–Se в частині $AgInSe_2$–$InSe$–Se за $T \leq 500$ К містить сім трифазних ділянок: In_2Se_3–$AgIn_{11}Se_{17}$–Se (I), $AgIn_{11}Se_{17}$–$AgIn_5Se_8$–Se (II), $AgIn_5Se_8$–$AgInSe_2$–Se (III), In_2Se_3–In_6Se_7–$AgIn_{11}Se_{17}$ (IV), In_6Se_7–$AgIn_{11}Se_{17}$–$AgIn_5Se_8$ (V), $InSe$–In_6Se_7–$AgIn_5Se_8$ та $InSe$–$AgIn_5Se_8$–$AgInSe_2$ (VI). Триангуляція $AgInSe_2$–$InSe$–Se встановлена за температурними залежностями ЕРС шести електрохімічних комірок (ЕХК) структури: (−) C | Ag | SE | R(Ag^+) | PE | C (+), де C – інертний електрод (графіт), Ag – негативний (лівий) електрод ЕХК, SE – твердий електроліт (скло Ag_3GeS_3Br), PE – позитивний (правий) електрод ЕХК, R(Ag^+) – ділянка PE, що контактує з SE, де за участі іонів Ag^+, як малих центрів зародження рівноважних фаз, відбувається перебудова фазово нерівноважної суміші сполук ПЕ зазначених в (I)–(VI) в термодинамічно стабільну суміш фаз. За температурними залежностями ЕРС комірок (*E*=*f*(*T*)) з ПЕ ділянок (I)–(VI) розраховано значення основних термодинамічних функцій бінарної In_6Se_7 та тернарних сполук у межуючих фазових ділянках за стандартних умов. Співпадіння значень енергії Ґіббса утворення сполуки $AgIn_5Se_8$ $\Delta_f G^{\circ}_{(II)}$=−(819,6 ± 8,9) кДж·моль$^{-1}$ та $\Delta_f G^{\circ}_{(V)}$=−(820,0 ± 8,9) кДж·моль$^{-1}$ розрахованих за *E*=*f*(*T*) з ПЕ ділянок (II), (V) характеризує фазовий склад ділянок (I), (II), (IV), (V) за $T \leq 500$ К як поєднання сполук формульного складу.

Ключові слова: срібловмісні сполуки, термодинамічні властивості, фазові рівноваги, енергія Ґіббса, метод ЕРС.